

## Key comparison BIPM.RI(I)-K3 of the air-kerma standards of the VSL, Netherlands and the BIPM in medium-energy x-rays

D.T. Burns and L.A. de Prez\*

Bureau International des Poids et Mesures, Pavillon de Breteuil, F-92312 Sèvres Cedex

\*Van Swinden Laboratorium BV, Thijssseweg 11, 2629 JA Delft

**Abstract** A key comparison has been made between the air-kerma standards of the VSL, Netherlands and the BIPM in the medium-energy x-ray range. The results show the standards to be in agreement at the level of the combined standard uncertainty when account is taken of the effect of the diaphragm support for the BIPM standard. The results are analysed and presented in terms of degrees of equivalence, suitable for entry in the BIPM key comparison database.

### 1. Introduction

An indirect comparison has been made between the air-kerma standards of the Van Swinden Laboratorium (VSL), Netherlands, and the Bureau International des Poids et Mesures (BIPM) in the x-ray range from 100 kV to 250 kV. Two cavity ionization chambers of type NE 2611 were used as transfer instruments. The measurements at the BIPM took place in November 2002 using the reference conditions recommended by the CCRI [1].

### 2. Determination of the air-kerma rate

For a free-air ionization chamber standard with measuring volume  $V$ , the air-kerma rate is determined by the relation

$$\dot{K} = \frac{I}{\rho_{\text{air}} V} \frac{W_{\text{air}}}{e} \frac{1}{1 - g_{\text{air}}} \prod_i k_i \quad (1)$$

where  $\rho_{\text{air}}$  is the density of air under reference conditions,  $I$  is the ionization current under the same conditions,  $W_{\text{air}}$  is the mean energy expended by an electron of charge  $e$  to produce an ion pair in air,  $g_{\text{air}}$  is the fraction of the initial electron energy lost through radiative processes in air, and  $\prod k_i$  is the product of the correction factors to be applied to the standard.

The values used for the physical constants  $\rho_{\text{air}}$  and  $W_{\text{air}}/e$  are given in Table 1. For use with this dry-air value for  $\rho_{\text{air}}$ , the ionization current  $I$  must be corrected for humidity and for the difference between the density of the air of the measuring volume at the time of measurement and the value given in the table<sup>1</sup>.

### 3. Details of the standards

Both free-air chamber standards are of the conventional parallel-plate design. The measuring volume  $V$  is defined by the diameter of the chamber aperture and the length of the collecting region. The BIPM air-kerma standard is described in [2] and the changes made to certain correction factors in October 2003 are given in [3] and the references therein. The VSL standard is described in [4] and was previously compared with the BIPM standard in an indirect

<sup>1</sup> For an air temperature  $T \sim 293$  K, pressure  $P$  and relative humidity  $\sim 50$  % in the measuring volume, this involves a temperature correction  $T/T_0$ , a pressure correction  $P_0/P$ , a humidity correction  $k_h = 0.9980$ , and the factor 1.0002 to account for the compressibility of dry air between  $T \sim 293$  K and  $T_0 = 273.15$  K.

comparison carried out in 1991 [5]. The main dimensions, the measuring volume and the polarizing voltage for each standard are shown in Table 2.

**Table 1. Physical constants used in the determination of the air-kerma rate**

Constant	Value	$u_i^a$
$\rho_{\text{air}}^b$	1.2930 kg m <sup>-3</sup>	0.000 1
$W_{\text{air}}/e$	33.97 J C <sup>-1</sup>	0.001 5

<sup>a</sup>  $u_i$  is the relative standard uncertainty.

<sup>b</sup> Density of dry air at  $T_0 = 273.15$  K and  $P_0 = 101.325$  kPa.

**Table 2. Main characteristics of the standards**

Standard	BIPM	VSL
Aperture diameter / mm	9.939	10.061
Air path length / mm	281.5	520
Collecting length / mm	60.004	100.37
Electrode separation / mm	180	300
Collector width / mm	200	340
Measuring volume / mm <sup>3</sup>	4 655.4	7 979.5
Polarizing voltage / V	4 000	6 000

## 4. The transfer instruments

### 4.1 Determination of the calibration coefficient for a transfer instrument

The air-kerma calibration coefficient  $N_K$  for a transfer instrument is given by the relation

$$N_K = \frac{\dot{K}}{I_{\text{tr}}} \quad (2)$$

where  $\dot{K}$  is the air-kerma rate determined by the standard using (1) and  $I_{\text{tr}}$  is the ionization current measured by the transfer instrument and the associated current-measuring system. The current  $I_{\text{tr}}$  is corrected to the standard conditions of air temperature, pressure and relative humidity chosen for the comparison ( $T = 293.15$  K,  $P = 101.325$  kPa and  $h = 50$  %).

For a BIPM comparison with a National Metrology Institute (NMI), the comparison result is defined as the BIPM air kerma determined by the NMI,  $K_{\text{NMI}}$ , relative to the reference value determined by the BIPM standard,  $K_{\text{R},i}$ .

To derive a comparison result from the calibration coefficients  $N_{K,\text{BIPM}}$  and  $N_{K,\text{NMI}}$  measured, respectively, at the BIPM and at an NMI, differences in the radiation qualities must be taken into account. Normally, each quality used for the comparison has the same nominal generating potential at each institute, but the half-value layers (HVLs) may differ. A radiation quality correction factor  $k_Q$  is derived for each comparison quality  $Q$ . This converts the calibration

coefficient  $N_{K,NMI}$  determined at the NMI into one which applies at the 'equivalent' BIPM quality and is derived by interpolation of the  $N_{K,NMI}$  values in terms of  $\log(\text{HVL})$ . For this indirect comparison, the comparison result,  $R_{K,NMI}$ , at each quality is then evaluated as

$$R_{K,NMI} = \frac{k_Q N_{K,NMI}}{N_{K,BIPM}} \quad (3)$$

In practice, the half-value layers normally differ by only a small amount and  $k_Q$  is close to unity.

#### 4.2 Details of the transfer instruments

Two thimble-type cavity ionization chambers belonging to the VSL were used as transfer instruments for the comparison. Their main characteristics are given in Table 3. Each chamber was oriented so that the text marked on the chamber stem was facing towards the source.

**Table 3. Main characteristics of the transfer chambers**

Chamber type	NE 2611	NE 2611
Serial number	116	117
Geometry	thimble	thimble
Reference point (on axis)	5 mm from tip	5 mm from tip
External diameter / mm	8.35	8.35
Polarizing potential <sup>a</sup> / V	+ 200	+ 200

<sup>a</sup> At the BIPM, the polarizing potential of + 200 V was applied to the thimble, the collecting electrode remaining at virtual ground potential. At the VSL, a potential of – 200 V was applied to the collecting electrode, the thimble remaining at ground potential.

## 5. Calibration at the BIPM

### 5.1 BIPM irradiation facility and reference radiation qualities

The BIPM high-voltage generator and x-ray tube for medium-energy x-rays were changed in June 2004. At the time of the comparison in 2002, the laboratory housed a constant-potential generator and a tungsten-anode x-ray tube with an inherent filtration of 2.3 mm aluminium. Both the generating potential and the tube current were stabilized using feedback systems constructed at the BIPM, resulting in a very high stability and obviating the need for a transmission current monitor. The radiation qualities used in the range from 100 kV to 250 kV are those recommended by the CCRI [1] and are given in Table 4.

The irradiation area is temperature controlled at around 20 °C and is stable over the duration of a calibration to better than 0.1 °C. Two thermistors, calibrated to a few mK, measure the temperature of the ambient air and the air inside the BIPM standard (which is controlled at 25 °C). Air pressure is measured by means of a calibrated barometer positioned at the height of the beam axis. The relative humidity is controlled within the range 47 % to 53 % and consequently no humidity correction is applied to the current measured using transfer instruments.

### 5.2 BIPM standard and correction factors

The reference plane for the BIPM standard was positioned at 1200 mm from the radiation source, with a reproducibility of 0.03 mm. The standard was aligned on the beam axis to an estimated uncertainty of 0.1 mm. The beam diameter in the reference plane was 83 mm for all radiation qualities.

**Table 4. Characteristics of the BIPM reference radiation qualities**

Radiation quality	100 kV	135 kV	180 kV	250 kV
Generating potential / kV	100	135	180	250
Additional Al filtration / mm	1.203	-	-	-
Additional Cu filtration / mm	-	0.232	0.485	1.570
Al HVL / mm	4.027	-	-	-
Cu HVL / mm	0.148	0.494	0.990	2.500
$\mu_{\text{air}}^{\text{a}} / \text{m}^{-1}$	0.0360	0.0238	0.0201	0.0174
$\dot{K}_{\text{BIPM}} / \text{mGy s}^{-1}$	0.21	0.20	0.29	0.38

<sup>a</sup> Air attenuation coefficient at 293.15 K and 101.325 kPa, measured at the BIPM for an air path length of 270 mm.

**Table 5. Correction factors for the BIPM standard**

Radiation quality	100 kV	135 kV	180 kV	250 kV	$u_{iA}$	$u_{iB}$
Air attenuation $k_a^{\text{a}}$	1.0102	1.0067	1.0057	1.0049	0.0003	0.0001
Scattered radiation $k_{\text{sc}}^{\text{b}}$	0.9952	0.9959	0.9964	0.9974	-	0.0003
Fluorescence $k_{\text{fl}}^{\text{b}}$	0.9985	0.9992	0.9994	0.9999	-	0.0003
Electron loss $k_e^{\text{b}}$	1.0000	1.0016	1.0043	1.0073	-	0.0009
Ion recombination $k_s$	1.0005	1.0005	1.0005	1.0005	0.0002	0.0001
Polarity $k_{\text{pol}}$	1.0002	1.0002	1.0002	1.0002	0.0001	-
Field distortion $k_d$	1.0000	1.0000	1.0000	1.0000	-	0.0007
Aperture edge transmission $k_l$	0.9999	0.9998	0.9997	0.9996	-	0.0001
Wall transmission $k_p$	1.0000	1.0000	0.9999	0.9988	0.0001	-
Humidity $k_h$	0.9980	0.9980	0.9980	0.9980	-	0.0003
$1 - g_{\text{air}}$	0.9999	0.9999	0.9998	0.9997	-	0.0001

<sup>a</sup> Values for 293.15 K and 101.325 kPa; each measurement is corrected using the air density measured at the time.

<sup>b</sup> Values for  $k_{\text{sc}}$ ,  $k_{\text{fl}}$  and  $k_e$  adopted in October 2003, based primarily on Monte Carlo calculations.

During the calibration of the transfer chambers, measurements using the BIPM standard were made using positive polarity only. A correction factor of 1.00015 was applied to correct for the known polarity effect in the standard. The leakage current for the BIPM standard, relative to the ionization current, was measured to be around  $2 \times 10^{-4}$ .

The correction factors applied to the ionization current measured at each radiation quality using the BIPM standard, together with their associated uncertainties, are given in Table 5.

The factor  $k_a$  corrects for the attenuation of the x-ray fluence along the air path between the reference plane and the centre of the collecting volume. It is evaluated using the measured air-attenuation coefficients  $\mu_{\text{air}}$  given in Table 4. In practice, the values used for  $k_a$  take account of the temperature and pressure of the air in the standard. Ionization current measurements (both for the standard and for transfer chambers) are also corrected for changes in air attenuation arising from variations in the temperature and pressure of the ambient air between the radiation source and the reference plane.

### 5.3 Transfer chamber positioning and calibration at the BIPM

The reference point for each chamber was positioned in the reference plane (1200 mm from the radiation source), with a reproducibility of 0.03 mm. Each transfer chamber was aligned on the beam axis to an estimated uncertainty of 0.1 mm.

The leakage current was measured before and after each series of ionization current measurements and a correction made using the mean value. The relative leakage current for both transfer chambers was around  $1 \times 10^{-3}$ .

For each transfer chamber and at each radiation quality, a set of seven measurements was made, each measurement with integration time 100 s. The relative standard uncertainty of the mean ionization current for each set was around  $2 \times 10^{-4}$ . Based on experience with other chambers of this type, an uncertainty component of  $3 \times 10^{-4}$  in relative value is introduced to account for the typical short-term reproducibility of chamber calibration coefficients for medium-energy x-rays at the BIPM.

## 6. Calibration at the VSL

### 6.1 VSL irradiation facility and reference radiation qualities

The medium-energy x-ray facility at the VSL comprises a constant-potential generator and a tungsten-anode x-ray tube with an inherent filtration of 4 mm beryllium. The generating potential has been calibrated using a high-purity germanium detector [4]. The short-term stability of the generating potential is better than 0.2 kV. The x-ray output is monitored by means of a transmission ionization chamber whose graphited Mylar<sup>TM</sup> windows introduce a filtration of less than  $5 \text{ mg cm}^{-2}$ . The short-term stability of the air-kerma rate relative to the transmission monitor is better than  $2 \times 10^{-4}$ . The characteristics of the VSL realization of the CCRI comparison qualities [1] are given in Table 6.

### 6.2 VSL standard and correction factors

The reference plane for the VSL standard was positioned at 1500 mm from the radiation source, with a reproducibility of 0.1 mm. The standard was aligned on the beam axis to an estimated uncertainty of 0.5 mm. The beam diameter in the reference plane is 123 mm for all radiation qualities.

During the calibration of the transfer chambers, measurements using the VSL standard were made using positive polarity only. No polarity correction has been applied. An uncertainty

component of  $3 \times 10^{-4}$  is included for the polarity effect. The relative leakage current was measured to be around  $3 \times 10^{-4}$ .

The correction factors applied to the ionization current measured at each radiation quality using the VSL standard, together with their associated uncertainties, are given in Table 7.

**Table 6. Characteristics of the VSL reference radiation qualities**

Radiation quality	100 kV	135 kV	180 kV	250 kV
Generating potential / kV	100	135	180	250
Additional Al filtration / mm	3.662	1.001	1.001	1.001
Additional Cu filtration / mm	-	0.305	0.598	1.748
Al HVL / mm	4.11	-	-	-
Cu HVL / mm	-	0.516	1.025	2.464
$\mu_{\text{air}}^{\text{a}} / \text{m}^{-1}$	0.0364	0.023 1	0.021 1	0.017 3
$\dot{K}_{\text{NMi VSL}} / \text{mGy s}^{-1}$	0.59	0.57	0.65	0.85

<sup>a</sup> Air attenuation coefficient at 293.15 K and 101.325 kPa, measured at the VSL for an air path length of 520 mm.

**Table 7. Correction factors for the VSL standard**

Radiation quality	100 kV	135 kV	180 kV	250 kV	$u_{iA}$	$u_{iB}$
Air attenuation $k_a^{\text{a}}$	1.019 1	1.012 1	1.011 0	1.009 0	-	0.001 0
Scattered radiation $k_{sc}$	0.992 1	0.993 4	0.994 4	0.995 7	-	0.002 0
Electron loss $k_e$	1.000 0	1.000 0	1.000 6	1.002 2	-	0.002 0
Ion recombination $k_s$	1.000 6	1.000 6	1.000 6	1.000 6	-	0.001 0
Polarity $k_{pol}$	1.000 0	1.000 0	1.000 0	1.000 0	-	0.000 3
Field distortion $k_d$	1.000 0	1.000 0	1.000 0	1.000 0	-	0.001 5
Aperture edge transmission $k_l$	0.999 9	0.999 8	0.999 5	0.999 2	-	0.000 6
Wall transmission $k_p$						
Humidity $k_h$	0.998 0	0.998 0	0.998 0	0.998 0	-	0.001 0
$1 - g_{\text{air}}$	1.000 0	1.000 0	1.000 0	1.000 0	-	0.000 2

<sup>a</sup> Nominal values for 293.15 K and 101.325 kPa; each measurement is corrected using the air density measured at the time.

The correction factor  $k_a$  is evaluated using the measured air-attenuation coefficients  $\mu_{\text{air}}$  given in Table 6. In practice, the values used for  $k_a$  take account of the temperature and pressure of the air

in the standard at the time of the measurements. Ionization measurements (standard and transfer chambers) are also corrected for variations in the temperature and pressure of the ambient air between the radiation source and the reference plane.

### 6.3 Transfer chamber positioning and calibration at the VSL

The reference point for each transfer chamber was positioned at the reference distance (at the VSL 1500 mm from the radiation source), with a reproducibility of 0.1 mm. Alignment on the beam axis was to an estimated uncertainty of 0.5 mm.

A calibrated thermistor was used to measure the air temperature. Air pressure was recorded using a calibrated barometer positioned at the height of the transfer chambers. The relative humidity in the VSL measurement area was in the range from 23 % to 28 %. No humidity correction has been applied to the current measured using the transfer instruments.

The leakage current was measured before and after each series of ionization current measurements and a correction made using the mean value. The relative leakage current for both transfer chambers was around  $2 \times 10^{-3}$ .

The relative standard uncertainty of the mean of a series of six measurements for each transfer chamber at each radiation quality was typically  $3 \times 10^{-4}$ . Based on the measurements before and after the chamber calibrations at the BIPM, an uncertainty component of  $1 \times 10^{-3}$  in relative value is introduced to account for the short-term reproducibility of the calibration coefficients determined at the VSL.

## 7. Additional corrections to transfer chamber measurements

### 7.1 Ion recombination, polarity, beam non-uniformity and field size

As can be seen from Tables 4 and 6, the air-kerma rates at the VSL are two to three times those at the BIPM. Thus volume recombination effects will be greater for the transfer chamber calibrations at the VSL, although no recombination corrections have been applied at either laboratory. An additional measurement was made at the BIPM at twice the usual air-kerma rate. The relative change in the calibration coefficient of  $2 \times 10^{-4}$  is within the statistical uncertainty of the measurement. Based on this, a relative uncertainty component of  $2 \times 10^{-4}$  is introduced. Each transfer chamber was used with the same polarity at each institute and so no correction is applied for polarity effects in the transfer chambers.

No correction is applied at either institute for the radial non-uniformity of the radiation field, which should be small for the transfer chambers used. The beam diameter at the VSL (123 mm) is significantly larger than the BIPM value (83 mm). It is known that transfer chambers respond to scattered radiation in a way that free-air chambers do not, so that calibration coefficients can show some sensitivity to field size. The magnitude of such an effect for small thimble-chamber types calibrated in medium-energy x-rays cannot at present be well estimated, but a relative standard uncertainty of  $1 \times 10^{-3}$  is introduced for this effect.

### 7.2 Radiation quality correction factors $k_Q$

As noted in Section 4.1, slight differences in radiation qualities may require a correction factor  $k_Q$ . From Tables 4 and 6 it is evident that the radiation qualities at the BIPM and at the VSL differ somewhat. By plotting the BIPM calibration coefficients  $N_{K,BIPM}$  as a function of the BIPM copper HVL values, values for  $k_Q$  were derived to convert the VSL calibration coefficients  $N_{K,VSL}$  to those that apply for the BIPM qualities (for the 100 kV quality, an estimate for the VSL copper HVL was derived from the aluminium HVL). The  $k_Q$  values so obtained are 0.9998, 0.9996, 0.9997 and 1.0001 for the four qualities 100 kV, 135 kV, 180 kV and 250 kV, respectively. The standard uncertainty of each of these factors is estimated to be  $1 \times 10^{-4}$ .

## 8. Uncertainties

The uncertainties associated with the primary standards are listed in Table 8, those for the transfer chamber calibrations in Table 9 and those for the comparison results in Table 10.

**Table 8. Uncertainties associated with the standards**

Standard	BIPM		VSL	
	$u_{iA}$	$u_{iB}$	$u_{iA}$	$u_{iB}$
Ionization current	0.000 3	0.000 2	0.001 0	0.000 6
Volume	0.000 1	0.000 5	-	0.001 5
Positioning	0.000 1	0.000 1	-	-
Correction factors (excl. $k_h$ )	0.000 4	0.001 2	-	0.003 6
Humidity $k_h$	-	0.000 3	-	0.001 0
Physical constants	-	0.001 5	-	0.001 5
$\dot{K}_{std}$	0.000 5	0.002 0	0.001 0	0.004 3

**Table 9. Uncertainties associated with the calibration of the transfer chambers**

Institute	BIPM		VSL	
	$u_{iA}$	$u_{iB}$	$u_{iA}$	$u_{iB}$
$\dot{K}_{std}$	0.000 5	0.002 0	0.001 0	0.004 3
Positioning of transfer chamber	0.000 1	0.000 1	-	0.001 0
$I_{tr}$	0.000 2	0.000 2	0.000 3	0.000 4
Short-term reproducibility	0.000 3	-	0.001 0	-
$N_{K, std}$	0.000 6	0.002 0	0.001 4	0.004 4

The combined standard uncertainty  $u_c$  of the comparison result takes into account correlations in the type B uncertainties associated with the physical constants and the humidity correction. Correlation in the BIPM and VSL values for  $k_c$  and  $k_{sc}$ , derived from Monte Carlo calculations in each laboratory, are taken into account in an approximate way by assuming half of the uncertainty value at each laboratory. This is consistent with the analysis of the results of BIPM comparisons in low-energy x-rays in terms of degrees of equivalence described in [6].

## 9. Results and discussion

The calibration coefficients determined at the BIPM and at the VSL are given in Table 11. The values given for the VSL are corrected using the  $k_Q$  values stated in Section 7.2. The results obtained for the two transfer chambers are in agreement at the level of around  $1.5 \times 10^{-3}$ , which

is consistent with the statistical uncertainty associated with current measurements and chamber positioning at the VSL.

**Table 10. Uncertainties associated with the comparison results**

Relative standard uncertainty	$u_{iA}$	$u_{iB}$
$N_{K,VSL}/N_{K,BIPM}$	0.0016	0.0035 <sup>a</sup>
Ion recombination	-	0.0002
Field size	-	0.0010
$k_Q$	-	0.0001
$\dot{K}_{VSL}/\dot{K}_{BIPM}$	$u_c = 0.0040$	

<sup>a</sup> Takes account of correlations in type B uncertainties.

**Table 11. Calibration coefficients for the transfer chambers**

Radiation quality	100 kV	135 kV	180 kV	250 kV
<i>Transfer chamber NE 2611 - 116</i>				
$N_{K,VSL} / \text{Gy } \mu\text{C}^{-1}$	90.55	91.01	91.55	92.01
$N_{K,BIPM} / \text{Gy } \mu\text{C}^{-1}$	90.39	91.19	91.82	92.65
Ratio VSL / BIPM	1.0017	0.9981	0.9971	0.9931
<i>Transfer chamber NE 2611 - 117</i>				
$N_{K,VSL} / \text{Gy } \mu\text{C}^{-1}$	90.67	91.22	91.66	92.06
$N_{K,BIPM} / \text{Gy } \mu\text{C}^{-1}$	90.41	91.21	91.81	92.57
Ratio VSL / BIPM	1.0028	1.0001	0.9983	0.9945

The comparison results  $R_{K,VSL}$  are summarized in Table 12. Comparing these results with those obtained for the comparison made in 1991, and taking account of the changes made to the BIPM standard in October 2003 documented in [3], consistency at the level of around  $5 \times 10^{-4}$  is obtained.

In absolute terms, it is clear from the final results (in bold) that there is a significant trend with radiation quality. This has been seen in a number of previous BIPM comparisons with other laboratories and the reason for this is now known. The diaphragm of the BIPM standard has an aluminium support that touches the outer surface of the diaphragm, the support itself having an aperture of diameter 12 mm and length 22 mm. It was identified recently that this support introduces significant scatter into the standard. This effect has now been measured for the four radiation qualities, giving correction factors to the BIPM standard of 0.9984(2), 0.9964(2), 0.9950(2) and 0.9935(2) at 100 kV, 135 kV, 180 kV and 250 kV, respectively. However, as the BIPM standard is the basis of the key comparison reference value, it cannot be changed without

the approval of the CCRI. This change will be documented in the open literature and implemented by the CCRI at the earliest opportunity. For this reason, the present report does not include these correction factors in the final comparison results. It should be noted that the degrees of equivalence between any pair of national laboratories remains independent of this future change (see Section 10).

When correcting for this effect the trend with radiation quality is significantly reduced, as seen in the final row of Table 12. The deviations from unity are consistent with the stated comparison uncertainty of  $4.0 \times 10^{-3}$  (Table 10). Part of the remaining trend might be due to the fact that no correction for fluorescence is applied to the VSL standard. The calculations of fluorescence reabsorption by Burns [7] for many standards, including the VSL standard, suggest correction factors  $k_{fl}$  of around 0.9983 at 100 kV and 0.9998 at 250 kV. Application of these factors would reduce the trend with energy to 2 parts in  $10^3$  and would also bring the comparison results closer to unity.

**Table 12. Comparison results**

Radiation quality	100 kV	135 kV	180 kV	250 kV
$R_{K,VSL}$	<b>1.0023</b>	<b>0.9991</b>	<b>0.9977</b>	<b>0.9938</b>
Previous result (1991) <sup>a</sup>	1.0029	0.9993	0.9968	0.9938
New result corrected for diaphragm support	1.0039	1.0027	1.0027	1.0003

<sup>a</sup> The results from 1991 are corrected for the changes made to the BIPM standard in October 2003, as documented in [3]

## 10. Degrees of Equivalence

The analysis of the results of BIPM comparisons in medium-energy x-rays in terms of degrees of equivalence is described in [6]. Following a decision of the CCRI, the BIPM determination of the air kerma is taken as the key comparison reference value, for each of the CCRI radiation qualities. It follows that for each NMI  $i$  having a BIPM comparison result  $R_{K,i}$  (denoted  $x_i$  in the KCDB) with combined standard uncertainty  $u_i$ , the degree of equivalence with respect to the reference value is given by a pair of terms: the relative difference  $D_i = (K_i - K_{R,i})/K_{R,i} = R_{K,i} - 1$  and its expanded uncertainty  $U_i = 2 u_i$ . The results for  $D_i$  and  $U_i$ , including those of the present comparison, are shown in Table 13 and in Figure 1, expressed in mGy/Gy as they are published in the BIPM key comparison database (KCDB). The results include those of an APMP comparison also published in the KCDB.

The degree of equivalence of NMI  $i$  with respect to each NMI  $j$  is the difference  $D_{ij} = D_i - D_j = R_{K,i} - R_{K,j}$  and its expanded uncertainty  $U_{ij} = 2 u_{ij}$ . In evaluating each  $u_{ij}$ , correlation between the standards is removed, notably that arising from the physical constants and from  $k_e$  and  $k_{sc}$ . As described in [6], if correction factors based on Monte Carlo calculations are used by both laboratories, or by neither, then half the uncertainty value is taken for each factor  $k_e$  and  $k_{sc}$ . Note that the uncertainty of the BIPM determination of air kerma does not enter in  $u_{ij}$ , although the uncertainty arising from the comparison procedure is included. The results for  $D_{ij}$  and  $U_{ij}$  when  $j$  represents the VSL are also given in Table 13 and in Figure 2. Note that the data presented in the tables, while correct at the time of publication of the present report, will become out-of-date as NMIs make new comparisons. The formal results under the CIPM MRA are those given in the KCDB.

## References

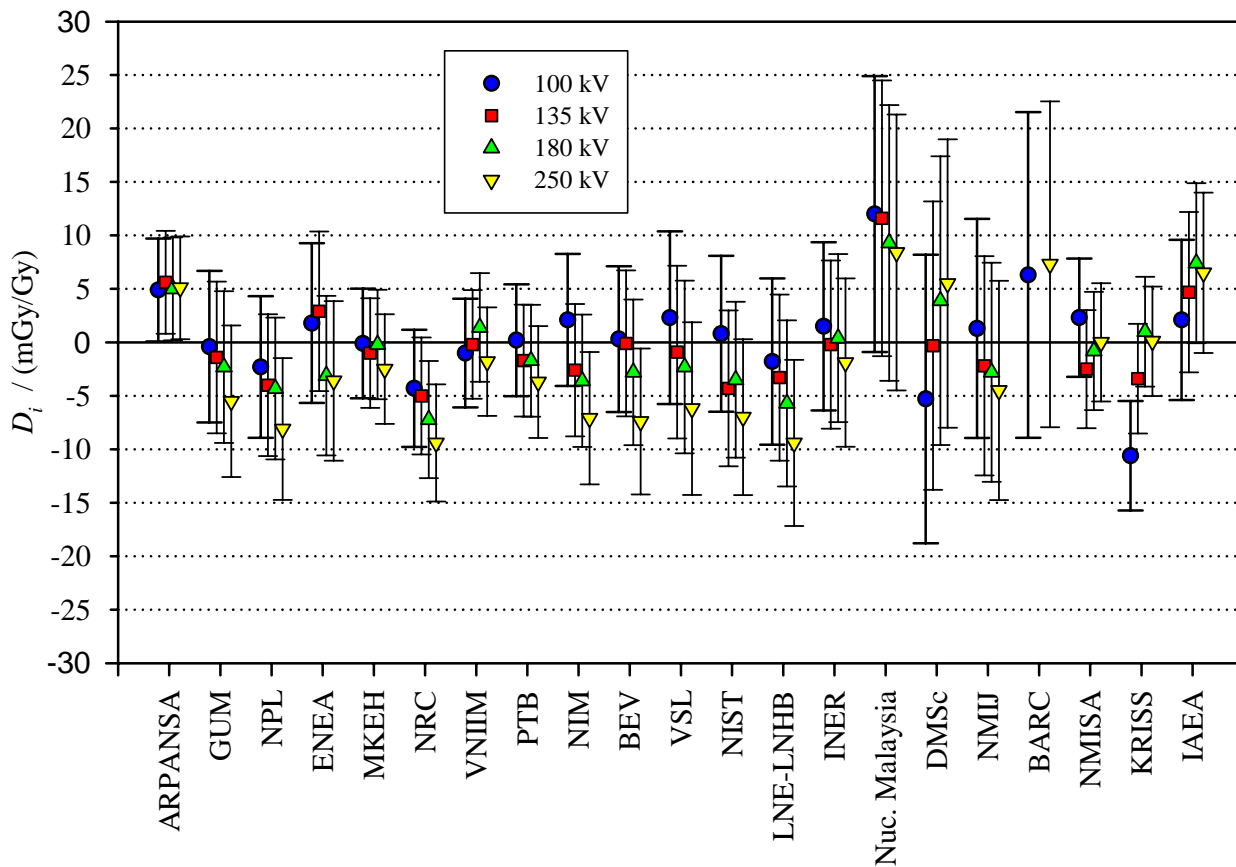
- [1] BIPM, Qualités de rayonnement, CCEMRI(I), 1972, R15.
- [2] BOUTILLON M., Mesure de l'exposition au BIPM dans le domaine des rayons X de 100 à 250 kV, 1978, [Rapport BIPM-78/3](#).
- [3] BURNS D.T., Changes to the BIPM primary air-kerma standards for x-rays, 2004, [Metrologia 41, L3](#).
- [4] GRIMBERGEN T.W.M., VAN DIJK E., DE VRIES W., Correction factors for the NMI free-air ionization chamber for medium-energy x-rays calculated with the Monte Carlo method, 1998, *Phys. Med. Biol.* **43** 3207–24
- [5] VAN DIJK E., GRIMBERGEN T.W.M., Report of the indirect comparison of kerma standards of BIPM and NMI December 1991, private communication.
- [6] BURNS D.T., Degrees of equivalence for the key comparison BIPM.RI(I)-K3 between national primary standards for medium-energy x-rays, 2003, [Metrologia 40 Technical Supplement, 06036](#).
- [7] BURNS D.T., Free-air chamber correction factors for electron loss, photon scatter, fluorescence and bremsstrahlung, 2001, [CCRI\(I\)/01-36](#).

Table 13. Degrees of equivalence. For each NMI  $i$ , the degree of equivalence with respect to the key comparison reference value is the difference  $D_i$  and its expanded uncertainty  $U_i$ , and with respect to NMI  $j$  is the difference  $D_{ij}$  and its expanded uncertainty  $U_{ij}$ . Here  $j$  represents the VSL. Tables formatted as they appear in the BIPM key comparison database.

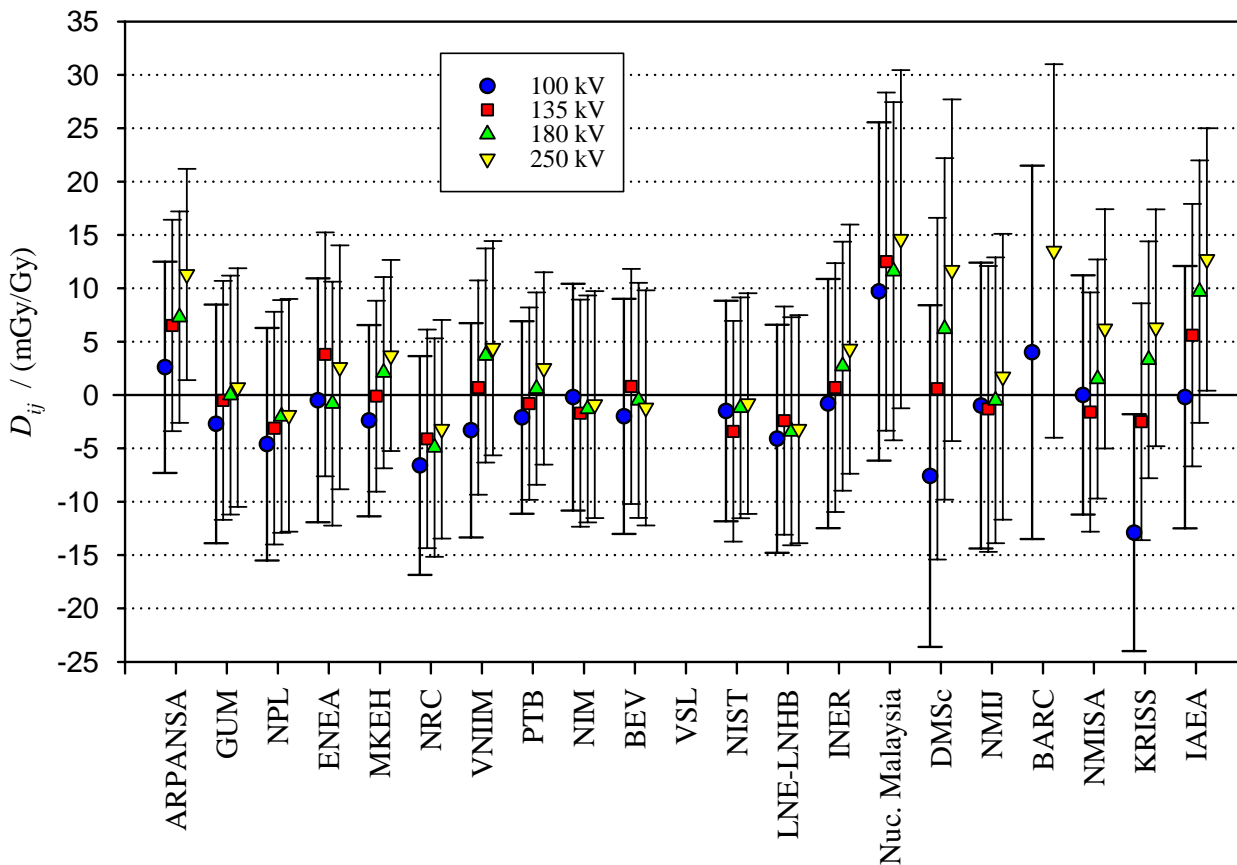
100 kV					135 kV				
NMI $i$	$D_i$	$U_i$	$D_{ij}$	$U_{ij}$	NMI $i$	$D_i$	$U_i$	$D_{ij}$	$U_{ij}$
	/(mGy/Gy)		/(mGy/Gy)			/(mGy/Gy)		/(mGy/Gy)	
ARPANSA	4.9	4.8	2.6	9.9	ARPANSA	5.6	4.8	6.5	9.9
GUM	-0.4	7.1	-2.7	11.2	GUM	-1.4	7.1	-0.5	11.2
NPL	-2.3	6.6	-4.6	10.9	NPL	-4.0	6.6	-3.1	10.9
ENEA	1.8	7.5	-0.5	11.4	ENEA	2.9	7.5	3.8	11.4
MKEH	-0.1	5.1	-2.4	9.0	MKEH	-1.0	5.1	-0.1	9.0
NRC	-4.3	5.5	-6.6	10.2	NRC	-5.0	5.5	-4.1	10.2
VNIIM	-1.0	5.1	-3.3	10.0	VNIIM	-0.2	5.1	0.7	10.0
PTB	0.2	5.2	-2.1	9.0	PTB	-1.7	5.2	-0.8	9.0
NIM	2.1	6.2	-0.2	10.6	NIM	-2.6	6.2	-1.7	10.6
BEV	0.3	6.8	-2.0	11.0	BEV	-0.1	6.8	0.8	11.0
VSL	2.3	8.1			VSL	-0.9	8.1		
NIST	0.8	7.3	-1.5	10.3	NIST	-4.3	7.3	-3.4	10.3
LNE-LNHB	-1.8	7.8	-4.1	10.7	LNE-LNHB	-3.3	7.8	-2.4	10.7
INER	1.5	7.9	-0.8	11.7	INER	-0.2	7.9	0.7	11.7
Nuc. Malaysia	12.0	12.9	9.7	15.8	Nuc. Malaysia	11.6	12.9	12.5	15.8
DMSc	-5.3	13.5	-7.6	16.0	DMSc	-0.3	13.5	0.6	16.0
NMIJ	1.3	10.2	-1.0	13.4	NMIJ	-2.2	10.2	-1.3	13.4
BARC	6.3	15.2	4.0	17.5	BARC				
NMISA	2.3	5.5	0.0	11.2	NMISA	-2.5	5.5	-1.6	11.2
KRISS	-10.6	5.1	-12.9	11.1	KRISS	-3.4	5.1	-2.5	11.1
IAEA	2.1	7.5	-0.2	12.3	IAEA	4.7	7.5	5.6	12.3

180 kV					250 kV				
NMI $i$	$D_i$	$U_i$	$D_{ij}$	$U_{ij}$	NMI $i$	$D_i$	$U_i$	$D_{ij}$	$U_{ij}$
	/(mGy/Gy)		/(mGy/Gy)			/(mGy/Gy)		/(mGy/Gy)	
ARPANSA	5.0	4.8	7.3	9.9	ARPANSA	5.1	4.8	11.3	9.9
GUM	-2.3	7.1	0.0	11.2	GUM	-5.5	7.1	0.7	11.2
NPL	-4.3	6.6	-2.0	10.9	NPL	-8.1	6.6	-1.9	10.9
ENEA	-3.1	7.5	-0.8	11.4	ENEA	-3.6	7.5	2.6	11.4
MKEH	-0.2	5.1	2.1	9.0	MKEH	-2.5	5.1	3.7	9.0
NRC	-7.2	5.5	-4.9	10.2	NRC	-9.4	5.5	-3.2	10.2
VNIIM	1.4	5.1	3.7	10.0	VNIIM	-1.8	5.1	4.4	10.0
PTB	-1.7	5.2	0.6	9.0	PTB	-3.7	5.2	2.5	9.0
NIM	-3.6	6.2	-1.3	10.6	NIM	-7.1	6.2	-0.9	10.6
BEV	-2.8	6.8	-0.5	11.0	BEV	-7.4	6.8	-1.2	11.0
VSL	-2.3	8.1			VSL	-6.2	8.1		
NIST	-3.5	7.3	-1.2	10.3	NIST	-7.0	7.3	-0.8	10.3
LNE-LNHB	-5.7	7.8	-3.4	10.7	LNE-LNHB	-9.4	7.8	-3.2	10.7
INER	0.4	7.9	2.7	11.7	INER	-1.9	7.9	4.3	11.7
Nuc. Malaysia	9.3	12.9	11.6	15.8	Nuc. Malaysia	8.4	12.9	14.6	15.8
DMSc	3.9	13.5	6.2	16.0	DMSc	5.5	13.5	11.7	16.0
NMIJ	-2.8	10.2	-0.5	13.4	NMIJ	-4.5	10.2	1.7	13.4
BARC					BARC	7.3	15.2	13.5	17.5
NMISA	-0.8	5.5	1.5	11.2	NMISA	0.0	5.5	6.2	11.2
KRISS	1.0	5.1	3.3	11.1	KRISS	0.1	5.1	6.3	11.1
IAEA	7.4	7.5	9.7	12.3	IAEA	6.5	7.5	12.7	12.3



**Figure 1.** Degrees of equivalence for each NMI  $i$  with respect to the key comparison reference value



**Figure 2.** Degrees of equivalence for each NMI  $i$  with respect to the VSL